Neuroinformatics (2019) 17:163–179
https://doi.org/10.1007/s12021-018-9389-6

SOFTWARE ORIGINAL ARTICLE

Towards Differential Connectomics with NeuroVIISAS

Sebastian Schwanke[1] · Jörg Jenssen[1] · Peter Eipert[1] · Oliver Schmitt[1]

Published online: 16 July 2018

Abstract

The comparison of connectomes is an essential step to identify changes in structural and functional neuronal networks. However, the connectomes themselves as well as the comparisons of connectomes could be manifold. In most applications, comparisons of connectomes are applied to specific sets of data. In many studies collections of scripts are applied optimized for certain species (non-generic approaches) or diseases (control versus disease group connectomes). These collections of scripts have a limited functionality which do not support functional and topographic mappings of connectomes (hemispherical asymmetries, peripheral nervous system). The platform-independent and generic *neuroVIISAS* framework is built to circumvent limitations that come with variants of nomenclatures, connectivity lists and connectional hierarchies as well as restrictions to structural connectome analyses. A new analytical module is introduced into the framework to compare different types of connectomes and different representations of the same connectome within a unique software environment. As an example a differential analysis of the partial connectome of the laboratory rat that is based on virus tract tracing with the same regions of non-virus tract tracing has been performed. A relatively large connectional coherence between the two different techniques was found. However, some detected connections are described by virus tract-tracing only.

Keywords Connectome · Differential connectomics · Neuronal networks · Multidimensional connectomes · Visualization · Graph analysis · Rat · Nervous system

Introduction

Since the first mappings of connectomes (Bailey et al. 1940; Felleman and Van Essen 1991) and the first quantitative analysis of a primate cortical visual connectome (Young 1992) the questions of connectomics have become more and more complex (Schmitt et al. 2017; Liu et al. 2011; Shen et al. 2017; Sporns 2011, 2012). This development is also due to the advantages of mathematical and analytical tools (Brandes and Erlebach 2005; Rubinov and Sporns 2010; Schmitt and Eipert 2012), network theory (Newman 2010; Jirsa and McIntosh 2007) as well as an enhanced network granularity (Zeng et al. 2015; Kuan et al. 2015; Oh et al. 2014) and quality (Kennedy et al. 2016). *Comparisons* of expression data are a fundamental analytical principle in the field of omics (Kobeissy et al. 2016; Kebschull et al. 2017; Wille et al. 2015a, b, 2017). Increasingly, connectomes are quantitatively compared to find explanations for structural or functional changes of connections and node properties under certain changes of experimental conditions or factors that may alter the architecture of connectomes (Hendricksen 2015). In line with the principle of multiple comparisons, a new module for differential connectome analysis has been implemented in *neuroVIISAS* (Schmitt and Eipert 2012) (http://neuroviisas.med.uni-rostock.de/neuroviisas.shtml). The term *differential connectomics* is used in the same manner as in other omics research (comparative omics, differential expression): differential proteomics (Anderle et al. 2004), comperative omics (Symons and Nieselt 2011; García-Alcalde et al. 2011; Kuo et al. 2013), comparative transcriptomics

✉ Oliver Schmitt
schmitt@med.uni-rostock.de

Sebastian Schwanke
sebastian.schwanke@uni-rostock.de

Jörg Jenssen
jc.jenssen@arcor.de

Peter Eipert
eipert@gmx.de

[1] Department of Anatomy, University of Rostock, Gertrudenstr. 9, 18057 Rostock, Germany

(Lawhorn et al. 2018). Differential connectomics is based on the comparison of connectome presentations (1) and analyses (2). Presentations in the form of matrices (adjacency matrices) which present neuronal connections and graphical visualizations of neuronal connections belong to the first category of differential connectomics. The second catergory of differential connectomics are computed relations between pairs of nodes (communicability matrix, connectivity matching matrix, generalized topology matrix, distance matrices etc.), gobal and local network parameters as well as motifs. The objective of a differential connectome analysis is the exploration of quantitative differences, visualization of changes and identification of similarities of different connectomes. In principle, comparisons of connectomes can be applied to different types of structural connectomes like complete connectomes (White et al. 1986), partial connectomes (Schmitt et al. 2012, 2016; Sukhinin et al. 2016; de Reus and van den Heuvel 2013; Bakker et al. 2012; Bota et al. 2005), isolated connectomes (Koelbl et al. 2015; Helmstädter et al. 2013; Helmstädter 2013; Oberländer et al. 2012) and functional connectomes (Xia and He 2017; Amico et al. 2017; Preti et al. 2016; Leonardi et al. 2013) as well as models of connectomes (Henriksen et al. 2016). So far, connectomes are built by a handful of techniques:

- histological high-throughput tract-tracing connectomes (HTC) (Oh et al. 2014; Zeng et al. 2015; Kuan et al. 2015),
- retrospective histological tract-tracing connectomes (RTC) (Schmitt et al. 2012, 2016; Wheeler et al. 2015; Bota et al. 2015; van den Heuvel et al. 2016; Swanson and Bota 2010; Swanson et al. 2016; Sugar et al. 2011; Scannell and Young 1993; Stephan et al. 2000, 2001 Sukhinin et al. 2016; de Reus and van den Heuvel 2013; Bakker et al. 2012),
- serial block-face scanning electron microscopy (SBEM) based microconnectomes (Wanner et al. 2015; Helmstädter et al. 2013; Helmstädter 2013; Oberländer et al. 2012),
- tractographic structural connectomes (TSC) (Rumple et al. 2013),
- functional fMRI connectomes (FMC) (Ma et al. 2017; Brynildsen et al. 2017; Paasonen et al. 2016; Bajic et al. 2016; Smith et al. 2016),
- molecular connectomes (MOC) (Livet et al. 2007; Tomer et al. 2014; Epp et al. 2015; Chung et al. 2013; Zador et al. 2012).

Connectomes are available at different spatial resolutions like microconnectomes (synaptic-level), mesoconnectomes (cortical-layer-level), macroconnectomes (region-subregion-level). Connectomes can be compared at all these resolutions. In a few cases, connectomes are organized in a hierarchy which allows sampling of regions and their connections through the branches of the hierarchy (cumulated links) (Schmitt and Eipert 2012). However, most comparisons are performed at a more or less unique level of organization of the nodes or regions of a connectome. Comparing connectomes of different species (interspecies and multiple-species connectomes (Wheeler et al. 2015)) is a further issue of differential connectomics. *neuroVIISAS* allows the administration of multiple connectome projects within a single instance of the framework (Schmitt and Eipert 2012). It turns out to be an optimal approach to compare different connectomes as well as variants of connectomes with regard to alternative nomenclatures and neuroontologies (Ding et al. 2016; Bota et al. 2005). A comparison to detect significant differences is a fundamental statistical concept (Yau 2013). An overview of some applications for comparing connectomes covers:

- **Human:** Comparisons of TSC, FMC (Lee et al. 2017)
  - **Health:** normal - diseased (van den Heuvel et al. 2012; Fornito et al. 2012; Dai et al. 2015; Cao et al. 2014; Gong and He 2015)
  - **Progress:** injury - treatment (Hannawi and Stevens 2016)
  - **Lateralization:** left - right (Caeyenberghs and Leemans 2014)
  - **Dimorphism:** female - male (Sun et al. 2015)
  - **Development:** young (Vértes and Bullmore 2015) - aged (Baker et al. 2015; Zuo et al. 2017; Collin and van den Heuvel 2013)
- **Intraspecies non-human:** Comparisons of HTC, RTC, SBEM, TSC, FMC, MOC
  - **Control-experiment:** Control organism connectome - experimentally modified organism connectome (Harris et al. 2016)
  - **Transgenic:** Control connectome - transgenetic connecteome (Daianu et al. 2015)
  - **Interregional:** intrinsic super-region connectome (e.g. thalamus) - other intrinsic super-region connectome (e.g., hypothalamus)
  - **Connectivity architectures:** direct connections of a connectome - cumulated connections of a hierarchical connectome
  - **Transsynaptic pathways:** Virus tract-tracing based connectome - non-virus based tract-tracing connectome
  - **Structure function relationship:** Functional connectomes - structural connectomes (Liang et al. 2018)
  - **Validation:** DTI-connectome - histological connectome (Gutman et al. 2012)

  - **Collation:** Intercollator comparisons of connectomes
  - **Dimorphism**
  - **Development**

- **Interspecies non-human:** HTC or TSC connectomes (Keifer et al. 2015)

Such a wide range of possibilities for comparing connectomes encouraged work on the design of a core functionality for differential connectome analysis in *neuroVIISAS*.

To demonstrate the principle of the analysis of different connectomes, the comparison of monosynaptic and transynaptic virus tract-tracing (Sizemore et al. 2016; Callaway and Luo 2015; Parr-Brownlie et al. 2015; Wouterlood et al. 2014; Ugolini 2011) connectivity data and non-viral monosynaptic tract-tracing (Mesulam 1982; Heilingoetter and Jensen 2016; Gerfen and Sawchenko 2016; Zaborszky et al. 2006) data of the laboratory rat were used. The motivation for this investigation is to detect coherent and differential connections of the virus- and the non-viral tract-tracing-methods. The results of the analysis could shed light on the problem of alternative routes of dense connectomes (Schmitt et al. 2016). Coherency of monosynaptic chains of connections (non-viral tract-tracing pathways) and transsynaptic pathways (virus tract-tracing) could support the selection of a specific route against a large amount of alternative routes through a directed connectome. The objective of this study is to present a novel extension of connectome analysis in the *neuroVIISAS* framework and to apply this new functionality of differential connectomics to the comparison of virus and non-viral based tract-tracing connectivity.

Methods

The connectivity data of strains of laboratory rats were manually curated in 7,400 peer-reviewed publications in which tract-tracing methods were applied. Because all connections as well as parameters of tract tracing experiments described in the texts, tables and figures need to be extracted an *in litero* extraction model could not be applied (Richardet et al. 2015; Gökdeniz et al. 2016; Vasques et al. 2015; French et al. 2015). Such an approach of generating a connectome is considered to be a metastudy (Crossley et al. 2016) or retrospective study as performed by many groups in the field (Young 1992; Sukhinin et al. 2016; Richardet et al. 2015; Bakker et al. 2012; Bota et al. 2005; Wheeler et al. 2015; Beul et al. 2015; Hilgetag et al. 2000; Scannell et al. 1995, 1999; Young et al. 1994; Scannell and Young 1993; Stephan et al. 2001, 2000). These publications were filtered from Pubmed (https://www.ncbi.nlm.nih.gov), GoogleScholar (https://scholar.google.com/), Scopus (https://www.scopus.com) and Web of Science (http://apps.webofknowledge.dom/). After matching the 4 database queries the references were imported into Jabref (http://jabref.sourceforge.net/) to obtain a unique and flexible bibtex style. The database has been continuously updated until now. Added references were immediately put into the pipeline of systematic curation. The database is available at http://neuroviisas.med.uni-rostock.de/references.html and can be queried by author names, e.g., "Swanson" would provide 114 references from a total of 25,202 (the author with most tract-tracing references in the rat connectome project). In order to automatically add new references to the database, it was allowed to leave multiple entries of same references due to different citation styles in the four databases or specific styles of the tools for citation export of publishers (used for publications which were accepted but not as fast available in Pubmed). As of now 25,202 references are available in the database. The bibtex database is loaded in *neuroVIISAS* within a particular project like the rat connectome project (http://neuroviisas.med.uni-rostock.de/connectome/index.php). E.g., the mouse connectome bibtex database is loaded when *neuroVIISAS* opens the mouse connectome project. Hence, the rat connectome database of references is constantly ("day by day") updated. This is an important requirement for comparing up-to-date connectomes. In addition to a complete database, the rat connectome project is built of ipsilateral and contralateral connectivity. For comparing viral tract-tracing connectivity with non-viral tract tracing results it is essential to consider supraspinal, spinal and peripheral nervous system connectivity. Furthermore, the connectivity data are not mixed with regard to species. However, they are mixed with regard to strains, sex and age. The regions, respectively, nodes of the connectome are organized in *variants* of the rat connectome ontology. This turns out to be useful since original publication based nomenclatures and terms are conserved. Modification of the nomenclature by just another expert has been prevented. For example, a *simplification* (cortical regions versus cortical layers), a *reorganization* (Paxinos cytoarchitectonic nomenclature (Paxinos and Watson 2014; Paxinos et al. 2015) versus Swanson ontogenetic nomenclature (Swanson 2004, 2014; Swanson and Bota 2010)) or a *matching* (Waxholm space nomenclature (Johnson et al. 2010; Zaslavsky et al. 2014; Papp et al. 2014) versus Paxinos nomenclature (Paxinos and Watson 2014; Paxinos et al. 2015)) was not necessary. Hence, the curation can remain as close as possible to the raw data of publications. The curator is not constrained to assign or interpret a vague or even missing definition of a region of a publication to a "standardized" atlas region. Experts in the field of subnuclei organization, definition of cortical transition regions and delineation of overlapping spatial definitions of cortical visual fields

(cf. (Paxinos and Watson 2014; Swanson 2004)) will find full support of *neuroVIISAS* for interactive reorganizing and modeling of nomenclatures and connectomes. In brief, the curation was performed as follows:

- the publication was printed out
- the curator underlines in the hardcopy species, sex and type of tracer
- the curator underlines in the hardcopy sources and targets of the connections that were documented either in tables, images or the text
- connections that were explicitly described in the texts, tables or images as *not found/not existent* were also marked
- if available all experiments or individual tracer injections which demonstrate a neuronal connection were collated

The data were conveyed to standardized spreadsheets (Excel or Calc) and exported as tab spaced csv files. The page numbers within the publications were assigned to each source-target-tuple. Furthermore, each source-target-tuple is built of a feature vector consisting of 25 elements (user-dependent) and each feature vector contains a unique bibtex-id to identify the underlying publication. To allow coding of transsynaptic virus propagation, the feature vectors which code monosynaptic parts of the virus pathway are linked by a modality item ("P": pathway indicator) and a connectivity logic: the target of a connection *must* be the source of the following monosynaptic part of the polysynaptic pathway. The last target of the monosynaptic chain or polysynaptic pathway is built of a feature vector without the "P" pathway indicator (stop signal). Axon colaterals are coded in a similiar way with a "C" colateral indicator. Ipsilateral connectivity is coded by "IPSI", contralateral by "CONTRA", unilateral connectivity by "LL" (left to left connection) or "RR" (right to right connection) or "LR" (left to right) or "RL", respectively which turns out to be necessary to code unilateral connectivity of the vegetative nervous system in the rat. Among different possibilities of data import into *neuroVIISAS* (quadratic connectivity matrix, BAMS-xml-file, GraphML-file, UMCD-UCLA-file and streamline file of DTI and tractographic data) the most simple form of a connection import is described in the following step by step: click on "File" in main window→ Create new Project → Continue → Continue → "test" project name → click on root node "test" in project frame → click on "Hierarchy" in main window → select "Import connections and create regions under selected node" → select the csv file. A simple csv file contains one connection per row with source region, target region and weight, e.g., A[TAB]B[TAB]{0, 1, 2, 3, 4}[CRLF]B[TAB]C[TAB]{0, 1, 2, 3, 4}[CRLF].... "A" is source region "A", "B" is traget region "B" followed by a value for the connection weight and then carriage return line feed (CRLF) and the second row with the connection from B to C follows. The default set of all values is documented in the help function or help.pdf of *neuroVIISAS*. Then proceed with "Analysis" → "Advanced connectivity analysis" double click on root node → "Refresh" button. Several connectome project files in the *neuroVIISAS* format are available on the *neuroVIISAS* webpage. The csv-file(s) may contain multiple collations of connections from different publications. They were imported into the rat connectome project and accumulated in the connectome database which can be exported directly from *neuroVIISAS* to a *mysql* database which is available online for the readership: http://neuroviisas.med.uni-rostock.de/connectome/index.php. Obviously, the virus-connectivity can be switched on or off by data-filtering within *neuroVIISAS* to allow an integration into or removal of non-viral tracer based connectivity. A core function of the framework is the *advanced connectivity analysis* (Figs. 1 and 3a). It activates an instance of a GUI for all aspects of connectome analysis (visual analytics, global network parameters, local network parameters, multivariate statistics (10 hierarchical clustering algorithms, multidimensional scaling, Kohonen self-organizing maps, principal component analysis, population simulations), community detection, motif analysis, vulnerability analysis, hub and rich-club analysis, 3D-visualization of analysis results, population-based simulations). Within an instance the regions of a connectome can be sampled. For a comparison more than one instance need to be opened (Figs. 1 and 3c and d). Several configurations can be realized for comparing connectomes (Fig. 1). The first possibility is to compare different types of a connectome of a particular project (Fig. 1a). A type of a connectome is a derivate of a connectome, which could differ with regard of selected regions, the selection of types of connections (direct or cumulated neuronal connections of a hierarchical organization of connections), the attributes of the neuronal connections or at least the selection of a surrogate (10 different models of network randomizations are available). More than two types of connectomes can be defined and used for differential comparisons. Each type of a connectome is an *instance* (Fig. 2). An example of 3 instances is shown in Fig. 1a. This first configuration of a differential connectome analysis is a *single project and multiple attributed connectomes* compilation (SPMC). The final selection of a pair of instances is done in the *differential matrix selection* (Fig. 3b) within the *differential analysis window*. A pairwise comparison has been realized, however, it is possible to open more than two instances to allow fast interactive switching between instances in the *differential analysis window* (Fig. 3b). The differential matrix displays quantitative values and/or qualitative information. A difference matrix which contains quantitative differences is shown in Fig. 3e. Differential values can

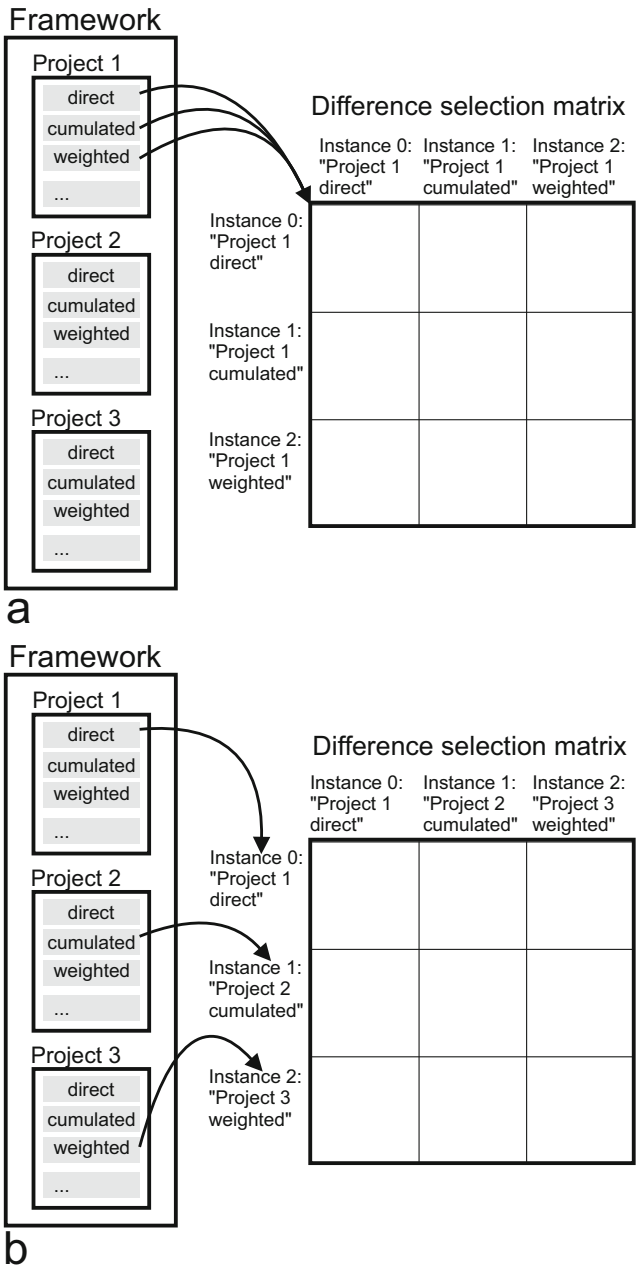

Fig. 1 Configurations of differential connectome analyses. Each connectome expresses a single instance. **a** Single project and multiple attributed connectomes (SPMC). **b** Multiple projects and multiple attributed connectomes (MPMC)

be distinguished from values of pairs of regions which occur in one instance, only (green filled circles: data occurs in the instance "Direct" but not in the instance "Cumulated"; blue filled circles: data occurs in the instance "Cumulated" but not in the instance "Direct". The degree of differences is color coded with square symbols and can be directly related to the instances which are coded by the same colors. If there exist no difference between values then the color white is assigned to the squares (Fig. 3e). Users are allowed to change color codes to improve visibility. Another possibility, e.g., for comparison of connectomes of different species, is the *multiple project multiple attributed connectomes* (MPMC) configuration. Different projects can be opened within a *neuroVIISAS* framework and types of connectomes can be defined in the *advanced connectivity analysis* function followed by transfer of the instances into the *differential analysis window* (Fig. 1b). In summary, the two configurations SPMC and MPMC are possible for comparing connectivity data of a single *neuroVIISAS* framework.

neuroVIISAS is a generic framework for digital atlasing, structural and functional connectome analysis, visualization and simulation. Simulations are possible by performing population models (NEST, http://www.nest-simulator.org/), coupled differential equtions (FitzHugh-Nagumo, Hindmarsh-Rose, Morris-Lecar, Kuramoto) in directed and weighted or binary connectomes, diffusion models (SER) and the Wilson-Cowan neural mass model. The module "differential connectivity analysis" (DCA) has been integrated into the framework. It is programmed in Java 1.6. The GUI of DCA is based on the GUI-Toolkit Swing which belongs to the Java foundation classes (JFC). In addition, the open source Java Swing docking framework DockingFrames (http://www.docking-frames.org/) was used to allow a more flexible design of the user interfaces. Furthermore, ColorBrewer functionality was used in DCA (http://colorbrewer2.org). The DCA window is based on the JFrame class. However, it is inherited from the "Advanced connectivity analysis" (ACA) window of *neuroVIISAS* (Fig. 2). An important feature is the dependence of DCA from ACA. If connectomes have been specified in more than one ACA instance, these instances can be recognized by DCA and configured in the compare control matrix of DCA (Fig. 2). Then a pairwise comparison of different data types like matrices, tables and motif configurations must be specified. An advantage of the implementation is the specification of matrices, tables, motifs and simulations (functional connectomics) in the ACA instances because the definitions of analyses could be complex. For example, in one instance an edge weighted connectome is defined by filtering only VTT connections. In the second instance, an edge-weighted connectome is defined where all edges have been detected by non-viral tract tracing methods, respectively, nVTT connectome. Then motif analyses should be performed on the VTT connectome from instance one and nVTT connectome from instance two. However, these analyses can be specified in more detail by adding customized microcircuits to the subgraph search and to select multiple null models (rewiring + Watts-Strogatz + Klemm-Eguílez etc.) for 10 to 10^4 iterations. More complex specifications concern functional connectomes with regard to varying parameters of coupled neuron models (FitzHugh-Nagumo, Hindmarsh-Rose, Morris-Lecar, Kuramoto etc.). Hence,

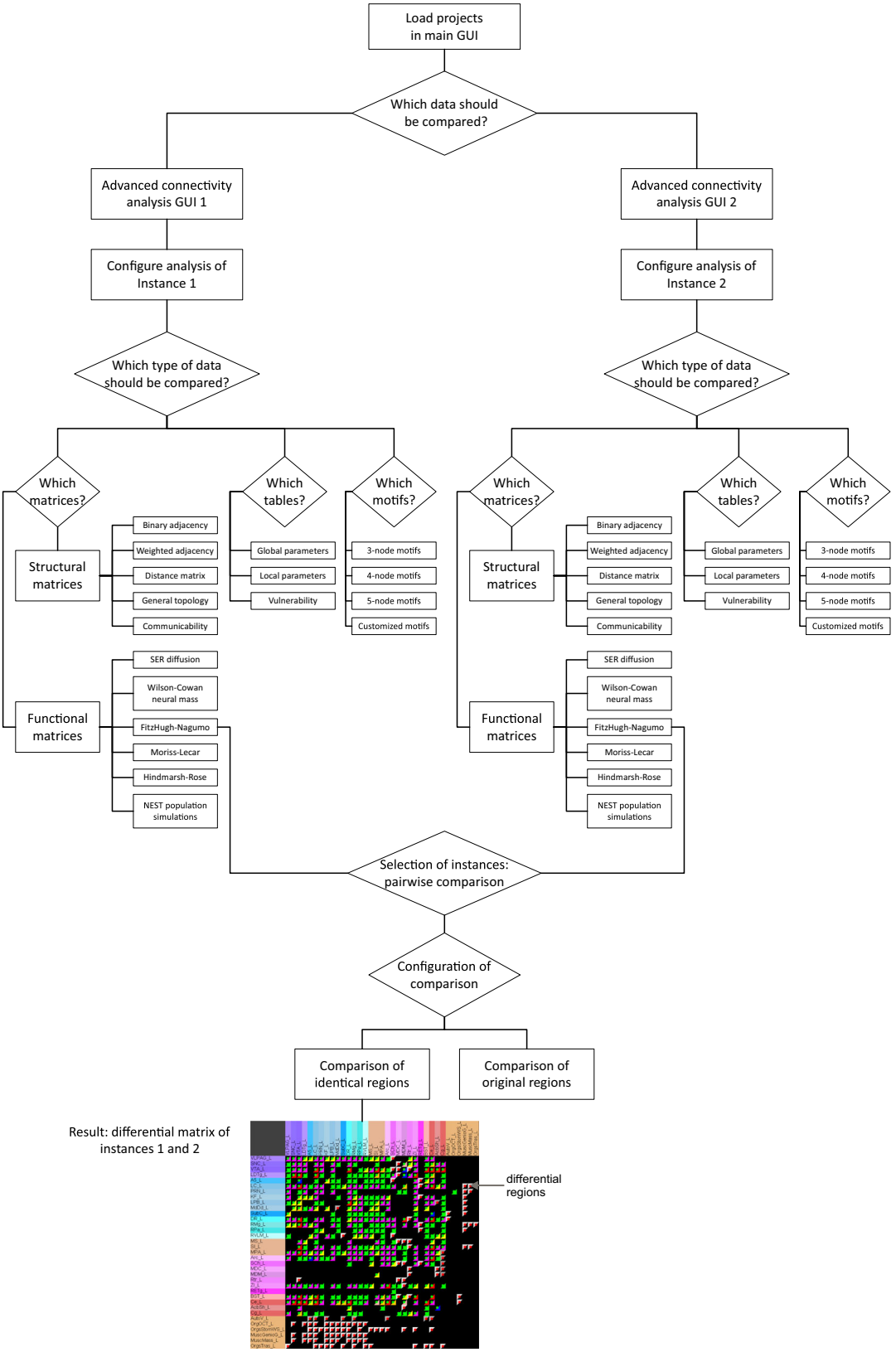

Fig. 2 Workflow of a differential connectome analysis. In this example, 2 instances are presented, however, more than 2 instances can be controlled by the compare control matrix (Fig. 3b). The gray arrow points to an extensive difference of connections of the VTT (instance 1) and nVTT (intance 2) in the differential results matrix. All symbols with a gray triangle and a red point indicate differences between a pair of regions (see gray arrow)

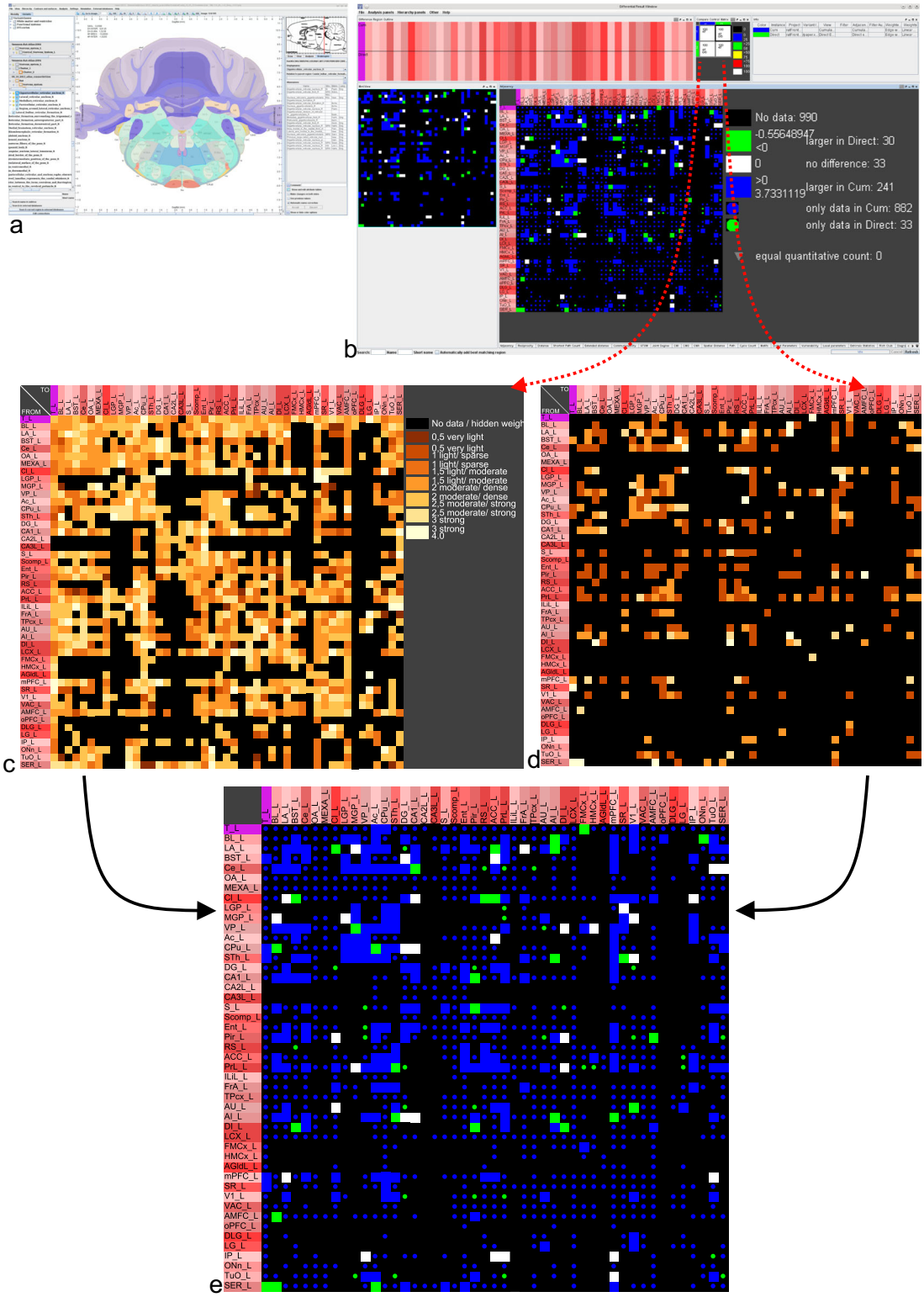

Fig. 3 Differential connectomes in distinct windows. **a** Main window of *neuroVIISAS*. **b** Differential analysis window with differential matrix. The red dashed arrows point to the *compare control matrix (CCM)*. In this case, instance 1 (Cum) and instance 2 (Direct) are selected and will be compared. Cumulated edges are connecting regions between nodes of subtrees and direct edges are connections between nodes, only. **c** Instance 1 window (semiquantitative weighted cumulated links). **d** Instance 2 window (semiquantitative weighted direct links). **e** The differential matrix for the instances "Cum" and "Direct". The legend of this matrix is shown in (**b**). The "Cum" instance has far more connections as indicated by blue filled circle (882). The "Direct" instance has 33 connections which do not occur in "Cum". 30 "Direct" connections have larger values than "Cum" and 241 connection have larger values in "Cum"

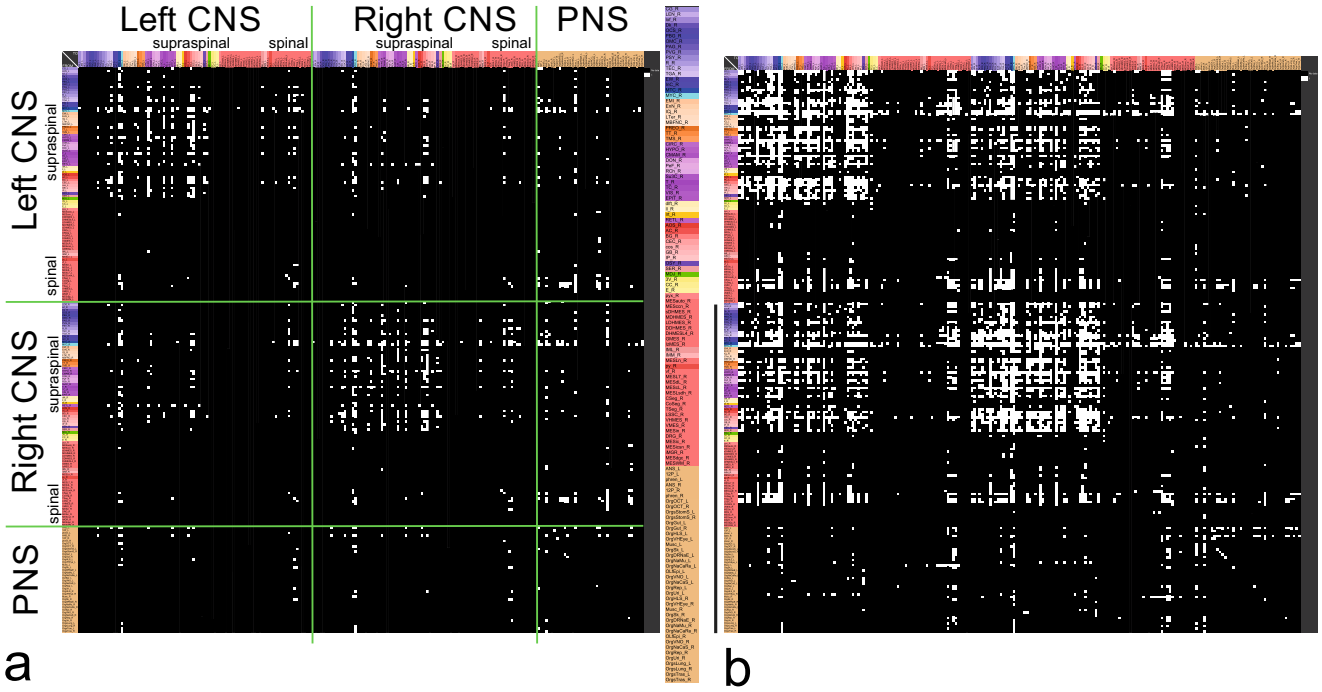

Fig. 4 **a** Viral tract tracing connectivity of direct and cumulated connections in a binary adjacency matrix. **b** Non-viral tract tracing connectivity. The adjacency matrix is binary and built of connections between visible regions (direct connections) as well as connections between not expanded branches of the hierarchy (cumulated connections). The black line marks those regions in the rows of the matrix which have been enlarged between the both matrices

instance dependent connectome definitions are flexible and the change of a connectome configuration is recognized by the DCA windows through listener technology. A differential connectome analysis has been visualized by a workflow (Fig. 2). In the workflow, 2 instances are shown and one differential matrix result with a significant number of regions and an obvious connectional difference of central and peripheral nervous systems connections (Fig. 2

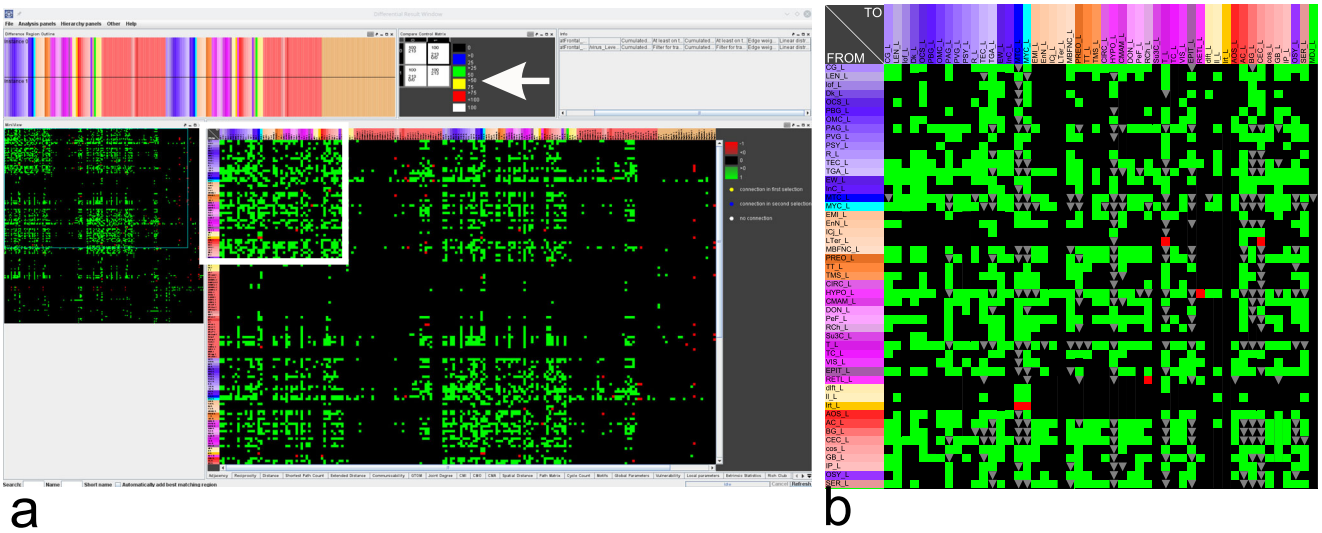

Fig. 5 Differential analysis window with the selected instance 0 (non-viral connectivity) and instance 1 (VTT-connectivity). The difference is calculated by [non-viral]-[VTT]. If the difference is larger than 0, the connection is non-viral and it is indicated by a green label. If the difference is smaller than 0, the connection is viral and it is indicated by a red label. Most connections are found or described by non-viral tract tracing. However, some connections (red) are found by virus-tract-tracing, only. **a** Main window of differential connectome analysis with the comparison control matrix (arrow). **b** Enlarged part of (**a**) with triangle coincidence markers. Green labels: connections that have been detected exclusively by non-viral tract tracing. Red labels: connections that have been detected exclusively by VTT. Gray triangles: coincident connections which were described by VTT and non-viral tract tracing

Table 1 Combinations of matrix element values in the differential adjacency matrix may provide loss of information

Instance 0	Instance 1	Numerical results					Matrix label
no data	no data	0	–	0	=	0	black
no data	not present	0	–	−10	=	10	green scale
not present	not present	−10	–	−10	=	0	red triangle
not present	exist	−10	–	1	=	−11	red scale
exist	not present	1	–	−10	=	11	green scale
exist	exist	1	–	1	=	0	gray triangle

arrow). However, more than two instances can be loaded in ACA and then added to the compare control matrix in DCA to interactively change the connectomes that are to be analyzed differentially. The very basic functionality is presented in the workflow, only. Parameter spaces, binary filter options, parameter selection processes as well as the flexibility of population definitions for the NEST simulator have been ignored in the workflow. Differential analysis of functional connectomes is limited to coactivation matrices (coupled neuron models) and spike coincidence matrices (population simulations). Furthermore, the workflow is cut off because differential graph visualization tools have been disregarded. The latest version of *neuroVIISAS* has been tested successfully on Microsoft Windows, Mac and Linux OS.

Results

The rat connectome project contains connections that were described by virus tract-tracing (VTT) of the peripheral and the central nervous system. Most of these VTT connections are monosynaptic, however, some connections were described as transsynaptic (multisynaptic, polysynaptic) with known intermediate neurons or regions describing a neuronal chain of transmission. However, most VTT transynaptic connections are documented by a source and target without determining intermediate regions and connections. Furthermore, most VTT connections were not characterized in the original publications by semiquantitative estimation of connection density or by stereological counting of the number of axons or measuring the optical density of labeled axons. The total number of ipsi- and contralateral VTT connections is 18,798 distributed over all branches of the hierarchy of the central and peripheral nervous system. These connections were collated out of

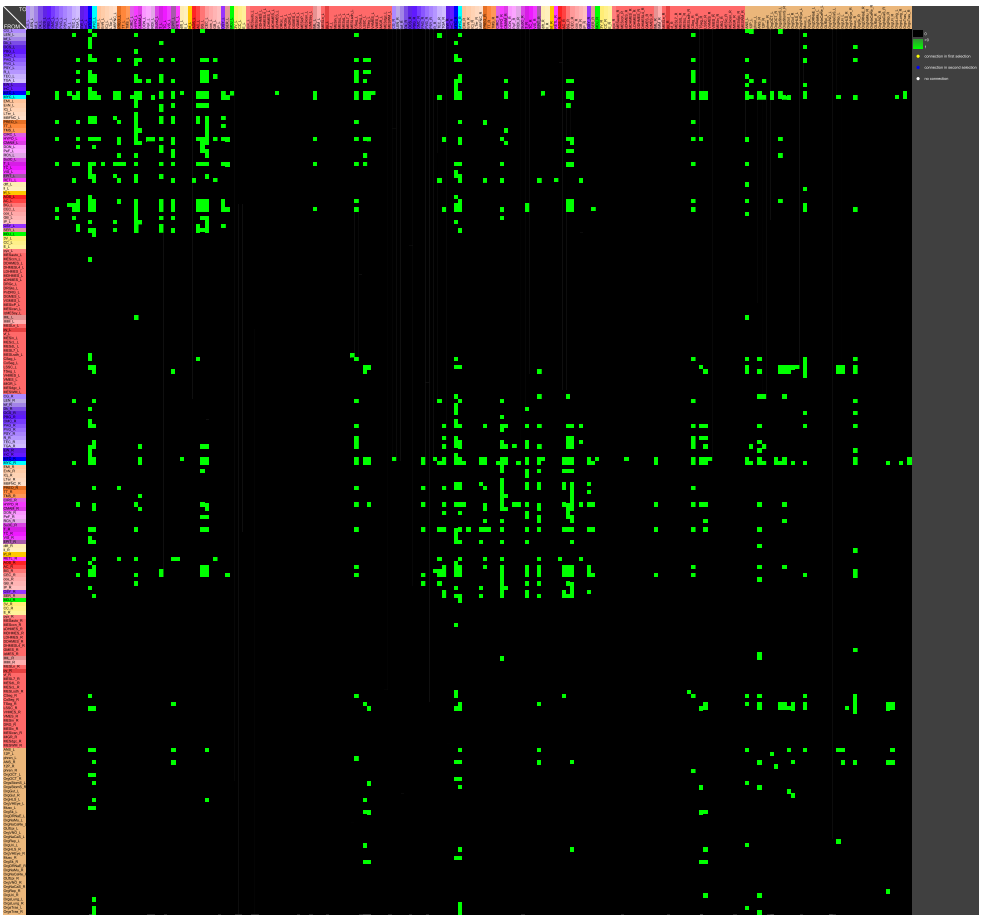

Fig. 6 The coincidence matrix results from the division of the two adjacency matrices of instance 0 and 1. If a connection is indicated in the non-viral tract tracing adjacency matrix as well as in the VTT adjacency matrix, then it is labeled by a green square in the coincidence matrix

363 different publications which describe at least one VTT experiment in the rat. In order to compare the VTT with the non-VTT connectivity, those regions were selected from the hierarchy which possess most VTT connections. The adjacency matrix of virus tract tracing consists of 213 regions connected by 1,095 links resulting in a line density of 2.42% (Fig. 4a). 220 reciprocal connections are realized and the average pathlength is 2.47.

The adjacency matrix of non-viral tract tracing consists of the same selection of regions which are connected by 5,097 links with a line density of 11.3%. 1,745 connections are reciprocal and the average pathlength is 2.04 (Fig. 4b). These adjacency matrices are binary and elements indicate direct connections or links between branches of the hierarchy. The selection of a pair of instances which are to be compared is performed in the compare control matrix (CCM) (Fig. 5a). The small control matrix provides the Jaccard indices or Jaccard similarity coefficients $J(A, B) = \frac{|A \cap B|}{|A \cup B|}$. Besides this default parameter further parameters can be switched to: Forbenius distance and correlation matrix measure (Herdin et al. 2005) of identical selections of regions of two instances. The matrix which shows the result of a comparison can be calculated for identical regions (identity matrix) and for identical regions and non-identical regions in combination with identical regions (Fig. 5b). Either the difference or the quotient between matrix elements is calculated. The contents of the matrices can be binary connections, weighted connections, number of experiments which have documented a connection. An attribute of a connection could be "no data" (no data available if a connection exists or not) and "non existent". If these attributes are assigned to a value of 0 and the matrix element is coded by a black matrix element label, then it is not possible to differentiate between several cases of a matrix element-connectivity property (Table 1):

Therefore, all three values of a connection can be differentiated by checkmarking the required cases. The VTT and non-VTT matrices are available in an instance 0 and instance 1 window. After loading all instances, the instances 0 and 1 are visible in the differential analysis window and the instances which should be compared were selected by the compare control matrix (Fig. 7a: white arrow).

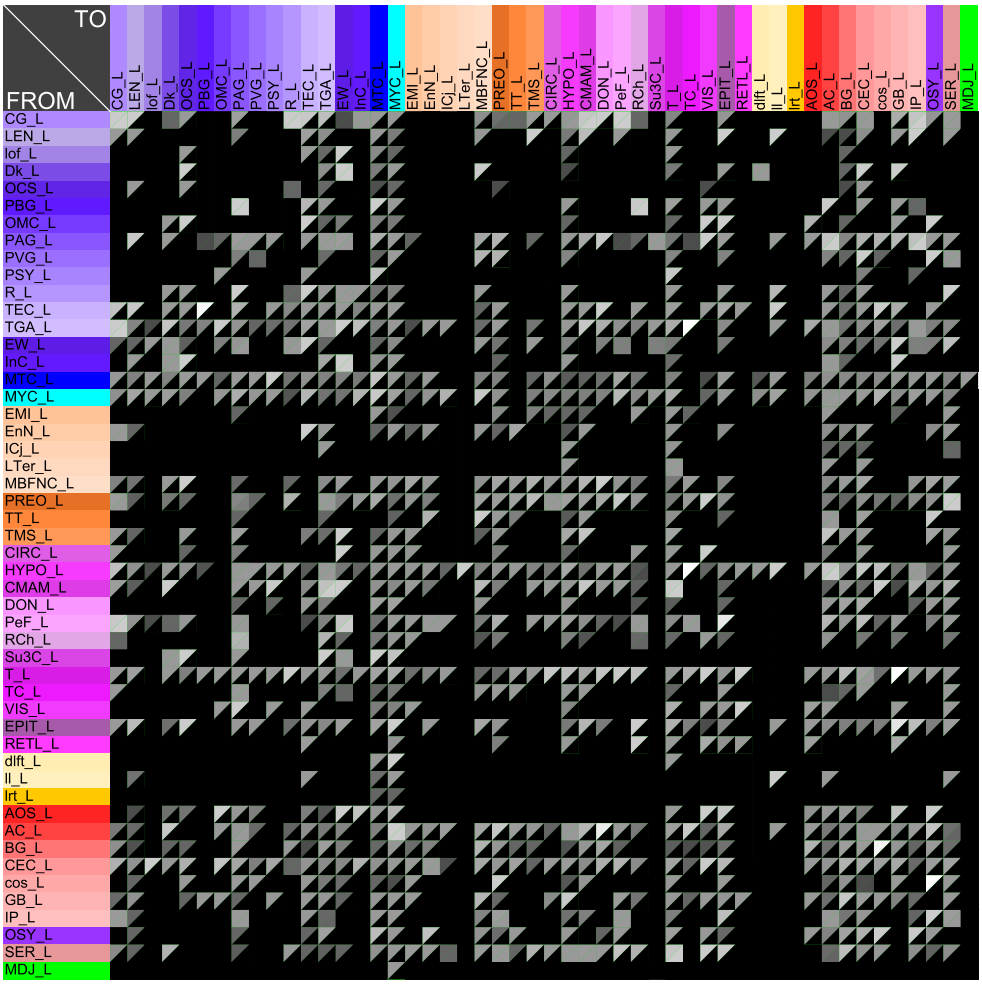

Fig. 7 The comparison matrix of absolute values of weights of two instances is magnified. The same part of the matrix has been cropped as in Fig. 5b. Upper corner triangles indicate connections of the first instance (cumulated edges) and lower corner triangles indicate connections of second instance (direct edges). A filled matrix element represents a connection of both instances

The differential adjacency matrix does not show coincidences of connections between the pairs of instances. The coincidences are calculated by the quotients of the two adjacency matrices (Fig. 6). 943 VTT-connections were detected by non-viral tract tracing as well. 137 VTT-connections were found exclusively by VTT. 4,286 connections were found exclusively by non-viral tract tracing.

Further differences and divisions of the matrices have been realized in the differential connectome analysis module of *neuroVIISAS*. A differential representation is available for the matrices of reciprocity, distance, shortest path count, extended distance (weighted distance), communicability, generalized topology, connectivity matching index (output, input, output+input) and the path matrix (connection between region through a chain of at least one intermediate region). To better compare the original matrix values of instances an *upper matrix element triangle* and *lower upper matrix element triangle* representation was added (Fig. 7). In this matrix the original values of, e.g., weights can be compared directly. If a triangle of a particular element of the matrix is filled in the upper left corner, then the connections occur in the first instance (cumulated edges) that was selected for comparison. If a triangle of a particular element of the matrix is filled in the lower right corner, then the connections occur in the second instance (direct connections) that was selected for comparison. If both triangles occur in one matrix element, then the connection exists in both instances. The same magnified part of the matrix shown in Fig. 5a is magnified in Fig. 5b.

Tables are a further group for the representation of analytical results of connectomes. Differential tables of global (Fig. 8) and local parameters (not shown) are available. The differential table of global parameters summarizes the original global parameters of instance 0 and 1, their difference, the magnitude, quotient and the relative increase, relative differences (instance 0 and 1 as well as instance 1 and 0). The average clustercoefficient increases by 27.4% and the average pathlength by 7.7% when comparing instance 0 (non-VTT) with instance 1 (VTT). The parameter of reciprocal connections provides a strong difference which is 1,715 in non-VTT instance 0 and 223 in VTT instance 1. In addition, differential tables of cycle count, vulnerability, rich club analysis and extrinsic connectivity are realized. A unique multiaxis representation of point processes allows the visualization of specific differential global parameters in relation to connectome surrogates of 8 randomization models (not shown). The same approach was used to differentially compare motif analysis results (Fig. 9). The frequency of 3-node motifs was determined in non-VTT instance 0 (red) and in the VTT instance 1 (blue). 8 different models of randomization were iterated 1000 times (Erdös Rényi (ER), Watts-Strogatz

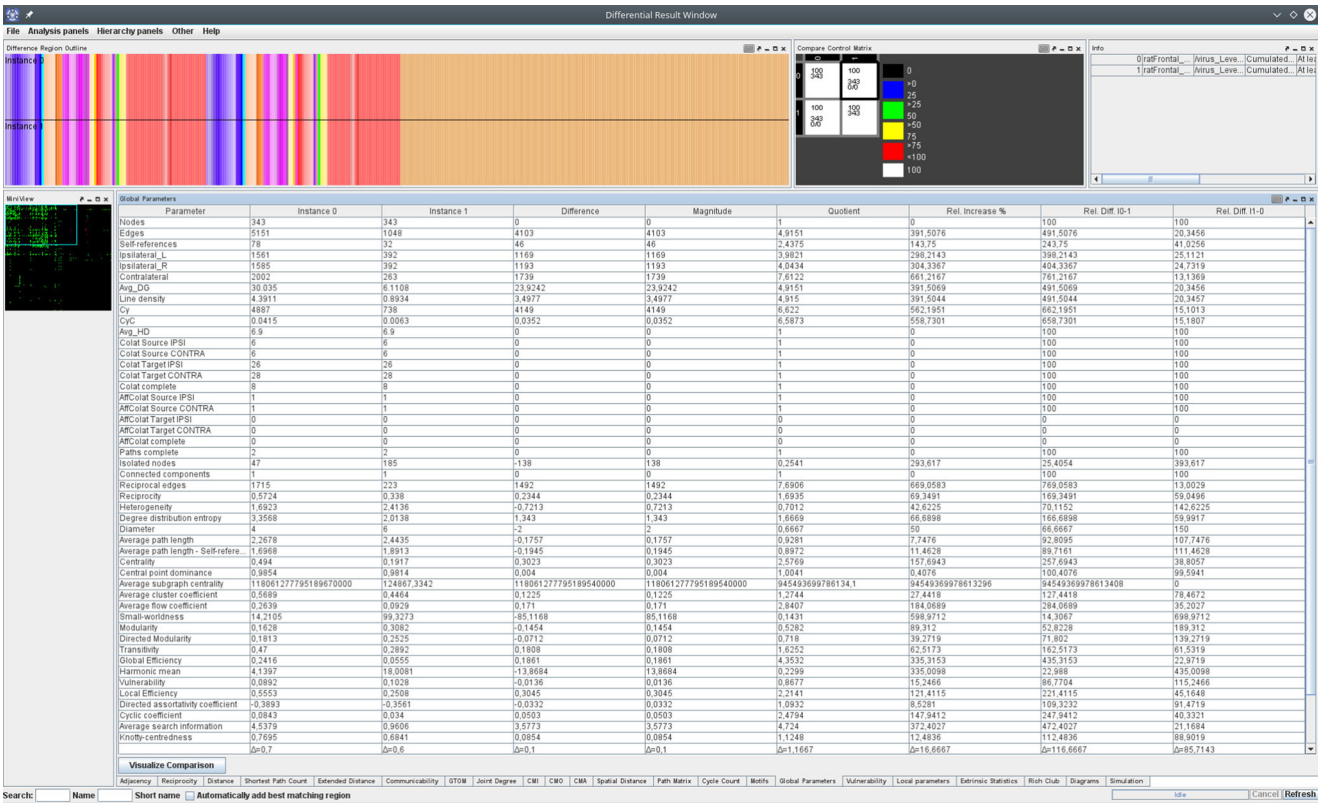

Fig. 8 Differential table of global network parameters. Original instance values are displayed and the absolute as well as relative differences

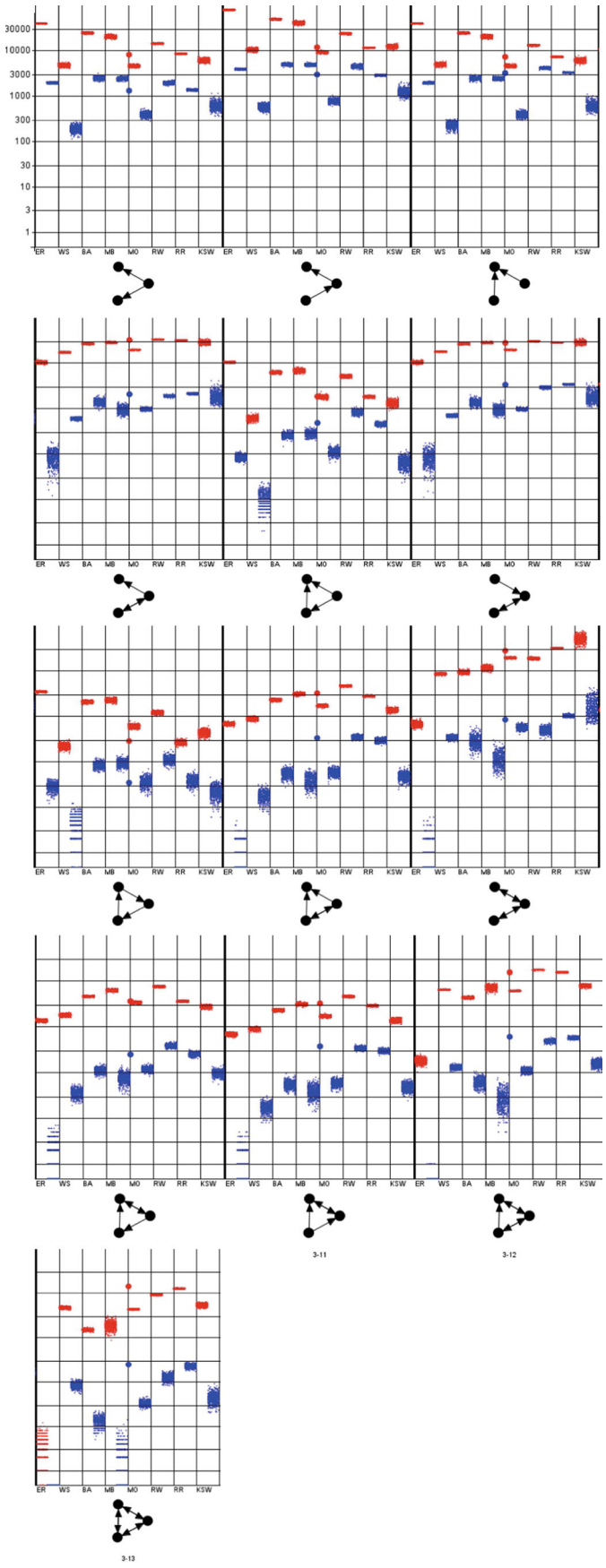

Fig. 9 Differential motif analysis. The relatively long continuous diagram has been splitted into 5 parts. The ordinate shows the logarithmic frequencies of the motifs. The red color indicates the non-VTT frequencies and the blue color the frequencies of VTT motifs. The 8 different randomizations models are shown on the abscissa. Small red dots indicate the frequencies of motifs in the randomization models of instance 1 (VTT) and blue dots of instance 0 (non-VTT). Randomization models are shown on the abscissa: Erdös Rényi (ER), Watts-Strogatz (WS), Barabasi-Albert (BA), modified Barabasi-Albert (MB), modified Oho (MO), rewiring (RW), rewiring with reciprocal edges (RR), Klemm-Eguílez (KSW)

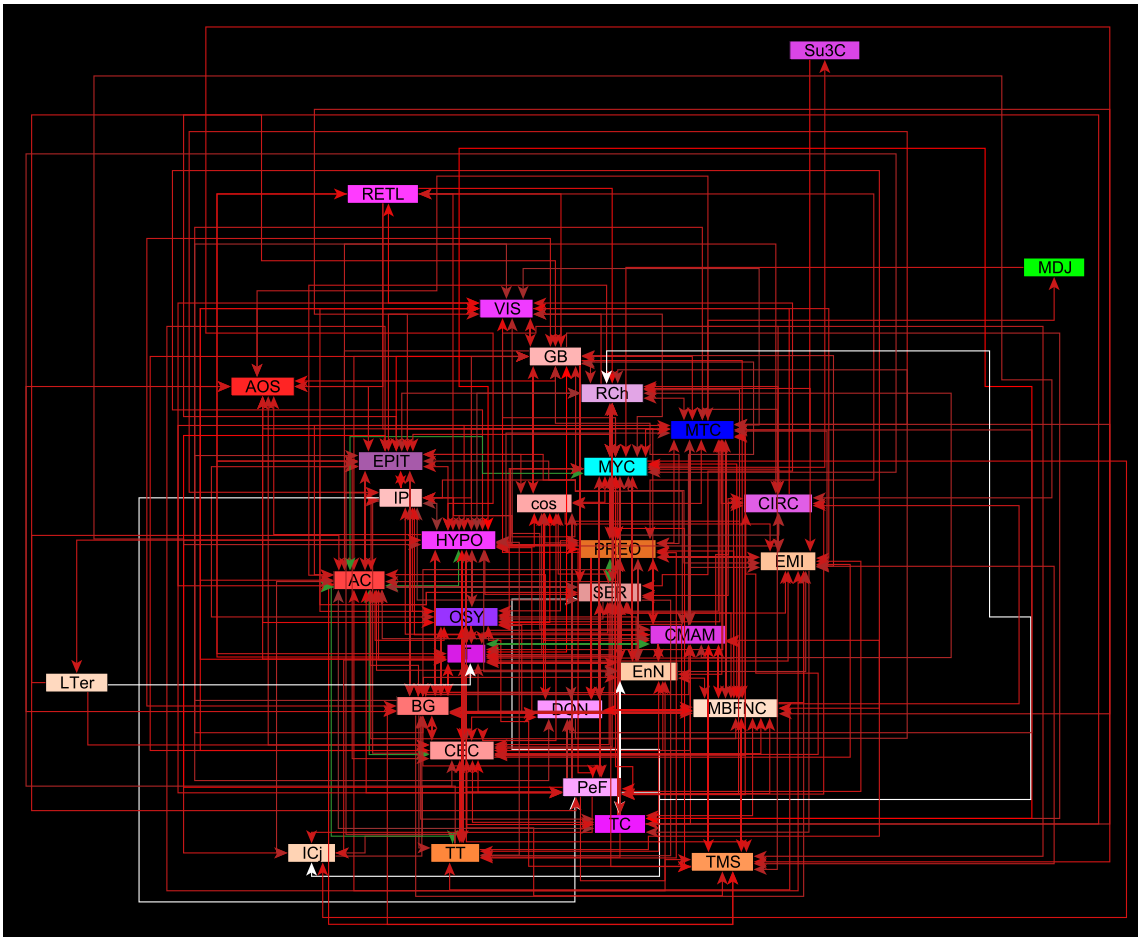

Fig. 10 Differential planar graph using bus router layout. Red connections occur in instance 1, only. Green connections occur in instance 2, only. White connections occur in both instances

(WS), Barabasi-Albert (BA), modified Barabasi-Albert (MB), modified Oho (MO), rewiring (RW), rewiring with reciprocal edges (RR), Klemm-Eguílez (KSW)) (Prettejohn et al. 2011). The frequency of a motif within a certain randomization model in instance 0 is indicated by a small red dot and in instance 1 by a small blue dot. Using this diagram, motif frequencies of the empirical models can easily be compared with randomization models. If the empirical frequency of a motif overlaps with the frequencies of a randomization model, then it does not differ from the randomization process or a randomization process is similar to the empirical data with regard to a particular motif. The rewiring randomization with the same number of reciprocal connections as in the empirical connectome is most similiar with the empirical connectome. The complete reciprocal motif 3–13 appears to be most different with regard to its frequency when comparing it with motif frequencies of randomizations. Differences of connections of two instances were visualized in a new type of graph visualization. This differential planar graph (Alper et al. 2013) represents all connections which possess differences when comparing two instances (Fig. 10). As an example the bus router layout, which is most common in visualizing neuronal connectivity in neuroanatomy (Shipp 2005; Felleman and Van Essen 1991), was chosen to demonstrate differential connectivity.

Discussion

It was shown that differential connectome analysis is realized in the generic framework of *neuroVIISAS*. A proof of principle was demonstrated by comparing two complex hierarchical connectomes of different modalities like non-VTT and VTT connectomes. The concept of multiple instances that are managed in a GUI for differential connectome analysis turned out to be flexible and scalable with regard to the number of pairwise comparisons among more than 2 instances. Different types of data representations were demonstrated like matrix comparison of identical regions and non-identical regions, table (global and local network parameters) comparisons and planar graph comparisons.

It was found that 137 connections were described exclusively by VTT methods and 943 coinciding connections of VTT and non-VTT were found indicating a relatively large confirmation of viral and non-viral detected connectivity. Nevertheless, viral connectivity with all its advantages and disadvantages compared to non-viral detected connectivity should be included in retrospective collator based connectome generation. The tract-tracing data that are based on transfections of neurotrophic viruses are strongly time-dependent. Especially those that, are derived from viruses which propagate transsynaptically. Therefore, these virus-based connections may reflect connectivity somewhere in between a highly specific monosynaptic connectivity up to a total infection or unspecific connectivity. Nevertheless, several experiments describe very clearly plausible transynaptic pathways which are also verified by stepwise non-virus tract-tracing methods. Certain functions of connectome analyses are comparative or differential like isomorphism search of a motif analysis. However, the results of a motif analysis can be considered differentially by comparing the results of motif frequencies of two different instances. Furthermore, the comparison of global parameters of a real connectome with different surrogates or models of randomization has been realized before in the form of a comparison table in the "Advanced connectivity analysis" module. In addition, the selection of regions of partial connectomes has been realized before within "Advanced connectivity analysis" module to obtain just an overview of complex connectomes. A problem that has not been addressed so far is the processing of a batch of comparisons. For example, the comparison of about 50 tractographic-based connectomes of normal individual with the tractographic based connectomes of 50 individuals suffering from psychiatric or neurological disorders. The export of matching regions of two connectomes is not a differential core function, however, it supports the work with pairs of connectomes. A matched connectome can simply be generated and analyzed independently from the differential analysis. For several years *neuoVIISAS* has undergone substantial extensions of its functionality. Because the differential analysis module uses analytical core functions of network and graph analysis it has been developed under the aspect of software extensibility. Added functions for graph analysis (randomization models, network parameters) are automatically recognized by the differential analysis module and become visible for the user (Alper et al. 2013). As an outlook new functions which should support visual analytical (Simoff et al. 2008; Dill et al. 2012; Gleicher et al. 2011) investigations like jo-jo visualization, transparent shifting (α-blending), false-color and backward-forward switching of a pair of instances is under development. Further progress will be made by implementing tools to perform stack or batch based differential analysis which is an important demand in comparing populations of DTI-connectomes from normal persons and diseased individuals.

Information Sharing Statement

The data and software in this study belong to an ongoing project. The latest releases of neuroVIISAS (RRID: SCR_006010) and example data are free to download from http://neuroviisas.med.uni-rostock.de/neuroviisas.shtml.

Acknowledgements We would like to thank Heidi Schumann and Christian Tominski (Computer Graphics, Institute of Computer Science, University of Rostock) for their helpful advice on the manuscript.

References

Alper, B., Bach, B., Riche, N.H., Isenberg, T., Fekete, J.-D. (2013). Weighted graph comparison techniques for brain connectivity analysis. In *Proceeding CHI '13 proceedings of the SIGCHI conference on human factors in computing systems* (pp. 483–492).

Amico, E., Marinazzo, D., Di Perri, C., Heine, L., Annen, J., Martial, C., Dzemidzic, M., Kirsch, M., Bonhomme, V., Laureys, S. (2017). Mapping the functional connectome traits of levels of consciousness. *Neuroimage*, *148*, 201–211.

Anderle, M., Roy, S., Lin, H., Becker, C., Joho, K. (2004). Quantifying reproducibility for differential proteomics: noise analysis for protein liquid chromatography-mass spectrometry of human serum. *Bioinformatics*, *20*, 3575–3582.

Bailey, P., De Barenne, J.C.D., Garol, H.W., McCulloch, W.S. (1940). Sensory cortex of chimpanzee. *Journal of Neurophysiology*, *3*, 469–485.

Bajic, D., Craig, M.M., Borsook, D., Becerra, L. (2016). Probing intrinsic Resting-State networks in the infant rat brain. *Frontiers in Behavioral Neuroscience*, *10*, 192.

Baker, S.T., Lubman, D.I., Yücel, M., Allen, N.B., Whittle, S., Fulcher, B.D., Zalesky, A., Fornito, A. (2015). Developmental changes in brain network hub connectivity in late adolescence. *Journal of Neuroscience*, *35*(24), 9078–9087.

Bakker, R., Wachtler, T., Diesmann, M. (2012). Cocomac 2.0 and the future of tract-tracing databases. *Frontiers in Neuroinformatics*, *27*(6), 30.

Beul, S.F., Grant, S., Hilgetag, C.C. (2015). A predictive model of the cat cortical connectome based on cytoarchitecture and distance. *Brain Structure and Function*, *220*(6), 3167–3184.

Bota, M., Dong, H.W., Swanson, L.W. (2005). Brain architecture management system. *Neuroinformatics*, *3*(1), 15–48.

Bota, M., Sporns, O., Swanson, L.W. (2015). Architecture of the cerebral cortical association connectome underlying cognition. *Proceedings of the National Academy of Sciences of the United States of America*, *112*(16), E2093–E2101.

Brandes, U., & Erlebach, T. (2005). *Network analysis. Methodological foundations. LNCS 3418*. Berlin: Springer.

Brynildsen, J.K., Hsu, L.M., Ross, T.J., Stein, E.A., Yang, Y., Lu, H. (2017). Physiological characterization of a robust survival rodent fMRI method. *Magnetic Resonance Imaging*, *35*, 54–60.

Caeyenberghs, K., & Leemans, A. (2014). Hemispheric lateralization of topological organization in structural brain networks. *Human Brain Mapping*, *35*(9), 4944–4957.

Callaway, E.M., & Luo, L. (2015). Monosynaptic circuit tracing with Glycoprotein-Deleted rabies viruses. *Journal of Neuroscience*, *35*(24), 8979–8985.

Cao, M., Shu, N., Cao, Q., Wang, Y., He, Y. (2014). Imaging functional and structural brain connectomics in attention-deficit/hyperactivity disorder. *Molecular Neurobiology*, *50*(3), 1111–1123.

Chung, K., Wallace, J., Kim, S.Y., Kalyanasundaram, S., Andalman, A.S., Davidson, T.J., Mirzabekov, J.J., Zalocusky, K.A., Mattis, J., Denisin, A.K., Pak, S., Bernstein, H., Ramakrishnan, C., Grosenick, L., Gradinaru, V., Deisseroth, K. (2013). Structural and molecular interrogation of intact biological systems. *Nature*, *497*(7449), 332–337.

Collin, G., & van den Heuvel, M.P. (2013). The ontogeny of the human connectome: development and dynamic changes of brain connectivity across the life span. *The Neuroscientist*, *19*(6), 616–628.

Crossley, N.A., Fox, P.T., Bullmore, E.T. (2016). Meta-connectomics: human brain network and connectivity meta-analyses. *Psychological Medicine*, *46*(5), 897–907.

Dai, Z., Yan, C., Li, K., Wang, Z., Wang, J., Cao, M., Lin, Q., Shu, N., Xia, M., Bi, Y., He, Y. (2015). Identifying and mapping connectivity patterns of brain network hubs in Alzheimer's disease. *Cerebral Cortex*, *25*(10), 3723–3742.

Daianu, M., Jacobs, R.E., Weitz, T.M., Town, T.C., Thompson, P.M. (2015). Multi-shell hybrid diffusion imaging (HYDI) at 7 Tesla in tgf344-AD transgenic Alzheimer rats. *PLoS One*, *10*(12), e0145205.

de Reus, M.A., & van den Heuvel, M.P. (2013). Rich club organization and intermodule communication in the cat connectome. *Journal of Neuroscience*, *33*(32), 12929–12939.

Dill, J., Earnshaw, R., Kasik, D., Vince, J., Wong, P.C. (2012). *Expanding the frontiers of visual analytics*. New York: Springer.

Ding, S.L., Royall, J.J., Sunkin, S.M., Ng, L., Facer, B.A., Lesnar, P., Guillozet-Bongaarts, A., McMurray, B., Szafer, A., Dolbeare, T.A., Stevens, A., Tirrell, L., Benner, T., Caldejon, S., Dalley, R.A., Dee, N., Lau, C., Nyhus, J., Reding, M., Riley, Z.L., Sandman, D., Shen, E., van der Kouwe, A., Varjabedian, A., Write, M., Zollei, L., Dang, C., Knowles, J.A., Koch, C., Phillips, J.W., Sestan, N., Wohnoutka, P., Zielke, H.R., Hohmann, J.G., Jones, A.R., Bernard, A., Hawrylycz, M.J., Hof, P.R., Fischl, B., Lein, E.S. (2016). Comprehensive cellular-resolution atlas of the adult human brain. *Journal of Comparative Neurology*, *524*(16), 3127–3481.

Epp, J.R., Niibori, Y., Liz Hsiang, H.L., Mercaldo, V., Deisseroth, K., Josselyn, S.A., Frankland, P.W. (2015). Optimization of CLARITY for clearing whole-brain and other intact organs. *eNeuro* 2(3), ENEURO.0022-15.2015.

Felleman, D.J., & Van Essen, D.C. (1991). Distributed hierarchical processing in the primate cerebral cortex. *Cerebral Cortex*, *1*, 1–47.

Fornito, A., Zalesky, A., Pantelis, C., Bullmore, E.T. (2012). Schizophrenia, neuroimaging and connectomics. *NeuroImage*, *62*(4), 2296–2314.

French, L., Liu, P., Marais, O., Koreman, T., Tseng, L., Lai, A., Pavlidis, P. (2015). Text mining for neuroanatomy using WhiteText with an upyeard corpus and a new web application. *Frontiers in Neuroinformatics*, *9*, 13.

García-Alcalde, F., García-López, F., Dopazo, J., Conesa, A. (2011). Paintomics: a web based tool for the joint visualization of transcriptomics and metabolomics data. *Bioinformatics*, *27*, 137–139.

Gerfen, C.R., & Sawchenko, P.E. (2016). An anterograde neuroanatomical tracing method that shows the detailed morphology of neurons, their axons and terminals: Immunohistochemical localization of an axonally transported plant lectin, Phaseolus vulgaris-leucoagglutinin (PHA-l). *Brain Research*, *1645*, 42–45.

Gleicher, M., Albers, D., Walker, R., Jusufi, I., Hansen, C.D., Roberts, J.C. (2011). Visual comparison for information visualization. *Information Visualization*, *10*(4), 289–309.

Gökdeniz, E., Özgür, A., Canbeyli, R. (2016). Automated neuroanatomical relation extraction: a linguistically motivated approach with a PVT connectivity graph case study. *Frontiers in Neuroinformatics*, *10*, 39.

Gong, Q., & He, Y. (2015). Depression, neuroimaging and connectomics: a selective overview. *Biological Psychiatry*, *77*(3), 223–235.

Gutman, D.A., Keifer, O.P., Magnuson, M.E., Choi, D.C., Majeed, W., Keilholz, S., Ressler, K.J. (2012). A DTI tractography analysis of infralimbic and prelimbic connectivity in the mouse using high-throughput MRI. *NeuroImage*, *63*(2), 800–811.

Hannawi, Y., & Stevens, R.D. (2016). Mapping the connectome following traumatic brain injury. *Current Neurology and Neuroscience Reports*, *16*(5), 44.

Harris, N.G., Verley, D.R., Gutman, B.A., Thompson, P.M., Yeh, H.J., Brown, J.A. (2016). Disconnection and hyper-connectivity underlie reorganization after TBI: a rodent functional connectomic analysis. *Experimental Neurology*, *277*, 124–138.

Heilingoetter, C.L., & Jensen, M.B. (2016). Histological methods for ex vivo axon tracing: a systematic review. *Neurological Research*, *38*(7), 561–569.

Helmstädter, M. (2013). Cellular-resolution connectomics: challenges of dense neural circuit reconstruction. *Nature Methods*, *10*(6), 501–507.

Helmstädter, M., Briggman, K.L., Turaga, S.C., Jain, V., Seung, H.S., Denk, W. (2013). Connectomic reconstruction of the inner plexiform layer in the mouse retina. *Nature*, *500*(7461), 168–174.

Hendricksen, R. (2015). Visualizing differences between brain networks. Eindhoven University of Technology, Department of Mathematics and Computer Science. Eindhoven, M.Sc. thesis.

Henriksen, S., Pang, R., Wronkiewicz, M. (2016). A simple generative model of the mouse mesoscale connectome. *Elife*, *5*, e12366.

Herdin, M., Czink, N., Özcelik, H., Bonek, H. (2005). Correlation matrix distance a meaningful measure for evaluation of non-stationary MIMO channels. In *IEEE Xplore conference vehicular technology conference* (Vol. 1, pp. 136–140).

Hilgetag, C.C., Burns, G.A., O'Neill, M.A., Scannell, J.W., Young, M.P. (2000). Anatomical connectivity defines the organization of clusters of cortical areas in the macaque monkey and the cat. *Philosophical Transactions of the Royal Society of London Series B: Biological Sciences*, *355*(1393), 91–110.

Jirsa, V.K., & McIntosh, A.R. (2007). *Handbook of brain connectivity*. Berlin: Springer.

Johnson, G.A., Badea, A., Brandenburg, J., Cofer, G., Fubara, B., Liu, S., Nissanov, J. (2010). Waxholm space: an image-based reference for coordinating mouse brain research. *NeuroImage*, *53*(2), 365–372.

Kebschull, M., Fittler, M.J., Demmer, R.T., Papapanou, P.N. (2017). Differential expression and functional analysis of high-throughput -omics data using open source tools. *Methods in Molecular Biology*, *1537*, 327–345.

Keifer, O.P., Gutman, D.A., Hecht, E.E., Keilholz, S.D., Ressler, K.J. (2015). A comparative analysis of mouse and human medial geniculate nucleus connectivity: a DTI and anterograde tracing study. *NeuroImage*, *105*, 53–66.

Kennedy, H., Van Essen, D.C., Christen, Y. (2016). *Micro- Meso- and Macro-connectomics of the brain*. Berlin: Springer.

Kobeissy, F.H., Guingab-Cagmat, J.D., Zhang, Z., Moghieb, A., Glushakova, O.Y., Mondello, S., Boutté, A.M., Anagli, J., Rubenstein, R., Bahmad, H., Wagner, A.K., Hayes, R.L., Wang, K.K. (2016). Neuroproteomics and systems biology approach to identify temporal biomarker changes post experimental traumatic brain injury in rats. *Frontiers in Neurology*, *7*, 198.

Koelbl, C., Helmstädter, M., Lübke, J., Feldmeyer, D. (2015). A barrel-related interneuron in layer 4 of rat somatosensory cortex with a high intrabarrel connectivity. *Cerebral Cortex*, *25*(3), 713–725.

Kuan, L., Li, Y., Lau, C., Feng, D., Bernard, A., Sunkin, S.M., Zeng, H., Dang, C., Hawrylycz, M., Ng, L. (2015). Neuroinformatics of the allen mouse brain connectivity atlas. *Methods*, *73*, 4–17.

Kuo, T.C., Tian, T.F., Tseng, Y.J. (2013). 3Omics: a web-based systems biology tool for analysis, integration and visualization of human transcriptomic, proteomic and metabolomic data. *BMC Systems Biology*, *7*, 64.

Lawhorn, C.M., Schomaker, R., Rowell, J.T., Rueppell, O. (2018). Simple comparative analyses of differentially expressed gene lists may overestimate gene overlap. *Journal of Computational Biology*, *25*(6), 606–612.

Lee, T.H., Miernicki, M.E., Telzer, E.H. (2017). Families that fire together smile together: Resting state connectome similarity and daily emotional synchrony in parent-child dyads. *NeuroImage*, *152*, 31–37.

Leonardi, N., Richiardi, J., Gschwind, M., Simioni, S., Annoni, J.M., Schluep, M., Vuilleumier, P., Van De Ville, D. (2013). Principal components of functional connectivity: a new approach to study dynamic brain connectivity during rest. *NeuroImage*, *83*, 937–950.

Liang, X., Hsu, L.M., Lu, H., Sumiyoshi, A., He, Y., Yang, Y. (2018). The Rich-Club Organization in rat functional brain network to balance between communication cost and efficiency. *Cerebral Cortex*, *28*(3), 924–935.

Liu, Y.Y., Slotine, J.J., Barabási, A.L. (2011). Controllability of complex networks. *Nature*, *473*(7346), 167–173.

Livet, J., Weissman, T.A., Kang, H., Draft, R.W., Lu, J., Bennis, R.A., Sanes, J.R., Lichtman, J.W. (2007). Transgenic strategies for combinatorial expression of fluorescent proteins in the nervous system. *Nature*, *450*(7166), 56–62.

Ma, Y., Hamilton, C., Zhang, N. (2017). Dynamic connectivity patterns in conscious and unconscious brain. *Brain Connect*, *7*(1), 1–12.

Mesulam, M.-M. (1982). *Tracing neural connections with horseradish peroxidase*. New York: Wiley.

Newman, M.E.J. (2010). *Networks*. Oxford: Oxford University Press.

Oberländer, M., de Kock, C.P., Bruno, R.M., Ramirez, A., Meyer, H.S., Dercksen, V.J., Helmstädter, M., Sakmann, B. (2012). Cell type-specific three-dimensional structure of thalamocortical circuits in a column of rat vibrissal cortex. *Cerebral Cortex*, *22*(10), 2375–2391.

Oh, S.W., Harris, J.A., Ng, L., Winslow, B., Cain, N., Mihalas, S., Wang, Q., Lau, C., Kuan, L., Henry, A.M., Mortrud, M.T., Ouellette, B., Nguyen, T.N., Sorensen, S.A., Slaughterbeck, C.R., Wakeman, W., Li, Y., Feng, D., Ho, A., Nicholas, E., Hirokawa, K.E., Bohn, P., Joines, K.M., Peng, H., Hawrylycz, M.J., Phillips, J.W., Hohmann, J.G., Wohnoutka, P., Gerfen, C.R., Koch, C., Bernard, A., Dang, C., Jones, A.R., Zeng, H. (2014). A mesoscale connectome of the mouse brain. *Nature*, *508*(7495), 207–214.

Paasonen, J., Salo, R.A., Huttunen, J.K., Gröhn, O. (2016). Resting-state functional MRI as a tool for evaluating brain hemodynamic responsiveness to external stimuli in rats. *Magnetic Resonance in Medicine*, *78*(3), 1136–1146.

Papp, E.A., Leergaard, T.B., Calabrese, E., Johnson, G.A., Bjaalie, J.G. (2014). Waxholm Space atlas of the Sprague Dawley rat brain. *NeuroImage*, *97*, 374–386.

Parr-Brownlie, L.C., Bosch-Bouju, C., Schoderboeck, L., Sizemore, R.J., Abraham, W.C., Hughes, S.M. (2015). Lentiviral vectors as tools to understand central nervous system biology in mammalian model organisms. *Frontiers in Molecular Neuroscience*, *8*, 14.

Paxinos, G., & Watson, C. (2014). *The rat brain in stereotaxic coordinates. 7 Aufl.* San Diego: Academic Press.

Paxinos, G., Watson, C., Calabrese, E., Badea, A., Johnson, G.A. (2015). *MRI/DTI Atlas of the rat brain*. San Diego: Academic Press.

Preti, M.G., Bolton, T.A., Van De Ville, D. (2016). The dynamic functional connectome: state-of-the-art and perspectives. *Neuroimage*, *S1053-8119*(16), 30788-1.

Prettejohn, B.J., Berryman, M.J., McDonnell, M.D. (2011). Methods for generating complex networks with selected structural properties for simulations: a review and tutorial for neuroscientists. *Frontiers in Computational Neuroscience*, *5*, 11.

Richardet, R., Chappelier, J.C., Telefont, M., Hill, S. (2015). Large-scale extraction of brain connectivity from the neuroscientific literature. *Bioinformatics*, *31*(10), 1640–1647.

Rubinov, M., & Sporns, O. (2010). Complex network measures of brain connectivity: uses and interpretations. *NeuroImage*, *52*, 1059–1069.

Rumple, A., McMurray, M., Johns, J., Lauder, J., Makam, P., Radcliffe, M., Oguz, I. (2013). 3-dimensional diffusion tensor imaging (DTI) atlas of the rat brain. *PLoS One*, *8*(7), e67334.

Scannell, J.W., & Young, M.P. (1993). The connectional organization of neural systems in the cat cerebral cortex. *Current Biology*, *3*(4), 191–200.

Scannell, J.W., Blakemore, C., Young, M.P. (1995). Analysis of connectivity in the cat cerebral cortex. *Journal of Neuroscience*, *15*(2), 1463–1483.

Scannell, J.W., Burns, G.A., Hilgetag, C.C., O'Neil, M.A., Young, M.P. (1999). The connectional organization of the cortico-thalamic system of the cat. *Cerebral Cortex*, *9*(3), 277–299.

Schmitt, O., & Eipert, P. (2012). NeuroVIISAS: approaching multiscale simulation of the rat connectome. *Neuroinformatics*, *10*(3), 243–267.

Schmitt, O., Eipert, P., Philipp, K., Kettlitz, R., Füllen, G., Wree, A. (2012). The intrinsic connectome of the rat amygdala. *Front Neural Circuits*, *6*, 81.

Schmitt, O., Eipert, P., Kettlitz, R., Lemann, F., Wree, A. (2016). The connectome of the basal ganglia. *Brain Structure and Function*, *221*(2), 753–814.

Schmitt, O., Badurek, S., Liu, W., Wang, Y., Rabiller, G., Kanoke, A., Eipert, P., Liu, J. (2017). Prediction of regional functional impairment following experimental stroke via connectome analysis. *Science Reports*, *7*, 46316.

Shen, X., Finn, E.S., Scheinost, D., Rosenberg, M.D., Chun, M.M., Papademetris, X., Constable, R.T. (2017). Using connectome-based predictive modeling to predict individual behavior from brain connectivity. *Nature Protocols*, *12*(3), 506–518.

Shipp, S. (2005). The importance of being agranular: a comparative account of visual and motor cortex. *Philosophical Transactions of the Royal Society of London Series B: Biological Sciences*, *360*(1456), 797–814.

Simoff, S.J., Böhlen, M.H., Mazeika, A. (2008). *Visual data mining. Theory, techniques and tools for visual analytics. Lecture notes in computer science 4404*. London: Springer.

Sizemore, R.J., Seeger-Armbruster, S., Hughes, S.M., Parr-Brownlie, L.C. (2016). Viral vector-based tools advance knowledge of basal ganglia anatomy and physiology. *Journal of Neurophysiology*, *115*(4), 2124–2146.

Smith, J.B., Liang, Z., Watson, G.D., Alloway, K.D., Zhang, N. (2016). Interhemispheric resting-state functional connectivity of the claustrum in the awake and anesthetized states. *Brain Structure and Function*, *222*(5), 2041–2058.

Sporns, O. (2011). *Networks of the brain*. Cambridge: The MIT Press.

Sporns, O. (2012). *Discovering the human connectome*. Cambridge: The MIT Press.

Stephan, K.E., Zilles, K., Kötter, R. (2000). Coordinate-independent mapping of structural and functional data by objective relational

transformation (ORT). *Philosophical Transactions of the Royal Society of London Series B: Biological Sciences*, *355*(1393), 37–54.

Stephan, K.E., Kamper, L., Bozkurt, A., Burns, G.A., Young, M.P., Kötter, R. (2001). Advanced database methodology for the Collation of Connectivity data on the Macaque brain (CoCoMac). *Philosophical Transactions of the Royal Society of London Series B: Biological Sciences*, *356*(1412), 1159–1186.

Sugar, J., Witter, M.P., van Strien, N.M., Cappaert, N.L.M. (2011). The retrosplenial cortex: intrinsic connectivity and connections with the (para)hippocampal region in the rat. An interactive connectome. *Frontiers in Neuroinformatics*, *5*, 7.

Sukhinin, D.I., Engel, A.K., Manger, P., Hilgetag, C.C. (2016). Building the ferretome. *Frontiers in Neuroinformatics*, *10*(10), 16.

Sun, Y., Lee, R., Chen, Y., Collinson, S., Thakor, N., Bezerianos, A., Sim, K. (2015). Progressive gender differences of structural brain networks in healthy adults: a longitudinal, diffusion tensor imaging study. *PLoS One*, *10*(3), e0118857.

Swanson, L.W. (2004). *Brain maps: Structure of the rat brain*, 3rd Edn. Amsterdam: Elsevier.

Swanson, L.W. (2014). *Neuroanatomical terminology. A lexicon of classical origins and historical foundations*. Oxford: Oxford University Press.

Swanson, L.W., & Bota, M. (2010). Foundational model of structural connectivity in the nervous system with a schema for wiring diagrams, connectome, and basic plan architecture. *Proceedings of the National Academy of Sciences of the United States of America*, *107*(48), 20610–20617.

Swanson, L.W., Sporns, O., Hahn, J.D. (2016). Network architecture of the cerebral nuclei (basal ganglia) association and commissural connectome. *Proceedings of the National Academy of Sciences of the United States of America*, *113*(40), E5972–E5981.

Symons, S., & Nieselt, K. (2011). MGV: a generic graph viewer for comparative omics data. *Bioinformatics*, *27*, 2248–2255.

Tomer, R., Ye, L., Hsueh, B., Deisseroth, K. (2014). Advanced CLARITY for rapid and high-resolution imaging of intact tissues. *Nature Protocols*, *9*(7), 1682–1697.

Ugolini, G. (2011). Rabies virus as a transneuronal tracer of neuronal connections. *Advances in Virus Research*, *79*, 165–202.

van den Heuvel, M.P., Sporns, O., Collin, G., Scheewe, T., Mandl, R.C., Cahn, W., Goñi, J., Hulshoff Pol, H.E., Kahn, R.S. (2012). Abnormal rich club organization and functional brain dynamics in schizophrenia. *JAMA Psychiatry*, *70*(8), 783–792.

van den Heuvel, M.P., Scholtens, L.H., de Reus, M.A. (2016). Topological organization of connectivity strength in the rat connectome. *Brain Structure and Function*, *221*, 1719–1736.

Vasques, X., Richardet, R., Hill, S.L., Slater, D., Chappelier, J.C., Pralong, E., Bloch, J., Draganski, B., Cif, L. (2015). Automatic target validation based on neuroscientific literature mining for tractography. *Frontiers in Neuroanatomy*, *9*, 66.

Verbeeck, N., Spraggins, J.M., Murphy, M.J., Wang, H.D., Deutch, A.Y., Caprioli, R.M., de Plas, R.V. (2017). Connecting imaging mass spectrometry and magnetic resonance imaging-based anatomical atlases for automated anatomical interpretation and differential analysis. *Biochimica et Biophysica Acta*, *S1570-9639*(17), 30040–30047.

Vértes, P.E., & Bullmore, E.T. (2015). Annual research review: Growth connectomics - the organization and reorganization of brain networks during normal and abnormal development. *Journal of Child Psychology and Psychiatry*, *56*(3), 299–320.

Wanner, A.A., Kirschmann, M.A., Genoud, C. (2015). Challenges of microtome-based serial block-face scanning electron microscopy in neuroscience. *Journal de Microscopie*, *259*(2), 137–142.

Wheeler, D.W., White, C.M., Rees, C.L., Komendantov, A.O., Hamilton, D.J., Ascoli, G.A. (2015). Hippocampome.org: a knowledge base of neuron types in the rodent hippocampus. *Elife*, *4*, e09960.

White, J.G., Southgate, E., Thomson, J.N., Brenner, S. (1986). The structure of the nervous system of the nematode Caenorhabditis elegans. *Philosophical Transactions of the Royal Society of London Series B: Biological Sciences*, *314*(1165), 1–340.

Wille, M., Schümann, A., Wree, A., Kreutzer, M., Glocker, M.O., Mutzbauer, G., Schmitt, O. (2015a). The proteome profiles of the cerebellum of juvenile, adult and aged rats - an ontogenetic study. *International Journal of Molecular Sciences*, *16*(9), 21454–21485.

Wille, M., Schümann, A., Kreutzer, M., Glocker, M.O., Wree, A., Mutzbauer, G., Schmitt, O. (2015b). The proteome profiles of the olfactory bulb of juvenile, adult and aged rats - an ontogenetic study. *Proteome Science*, *15*(13), 8.

Wille, M., Schümann, A., Kreutzer, M., Glocker, M.O., Wree, A., Mutzbauer, G., Schmitt, O. (2017). Differential proteomics of the cerebral cortex of juvenile, adult and aged rats - an ontogenetic study. *Journal of Proteomics and Bioinformatics*, in press.

Wouterlood, F.G., Bloem, B., Mansvelder, H.D., Luchicchi, A., Deisseroth, K. (2014). A fourth generation of neuroanatomical tracing techniques: exploiting the offspring of genetic engineering. *Journal of Neuroscience Methods*, *235*, 331–348.

Xia, M., & He, Y. (2017). Functional connectomics from a "big data" perspective. *Neuroimage*, *S1053-8119*(17), 30142-8.

Yau, N. (2013). *Data points: visualizing that means something*. Indianapolis: Wiley.

Young, M.P. (1992). Objective analysis of the topological organization of the primate cortical visual system. *Nature*, *358*(6382), 152–155.

Young, M.P., Scannell, J.W., Burns, G.A., Blakemore, C. (1994). Analysis of connectivity: neural systems in the cerebral cortex. *Reviews in the Neurosciences*, *5*(3), 227–250.

Zaborszky, L., Wouterlood, F.G., Lancietgo, J.L. (2006). *Neuroanatomical tract-tracing 3. Molecules, neurons and systems*. Singerpore: Springer.

Zador, A.M., Dubnau, J., Oyibo, H.K., Zhan, H., Cao, G., Peikon, I.D. (2012). Sequencing the connectome. *PLoS Biology*, *10*(10), e1001411.

Zaslavsky, I., Baldock, R.A., Boline, J. (2014). Cyberinfrastructure for the digital brain: spatial standards for integrating rodent brain atlases. *Frontiers in Neuroinformatics*, *8*, 74.

Zeng, T., Chen, H., Fakhry, A., Hu, X., Liu, T., Ji, S. (2015). Allen mouse brain atlases reveal different neural connection and gene expression patterns in cerebellum gyri and sulci. *Brain Structure and Function*, *220*(5), 2691–703.

Zuo, X.N., He, Y., Betzel, R.F., Colcombe, S., Sporns, O., Milham, M.P. (2017). Human connectomics across the life span. *Trends in Cognitive Sciences*, *21*(1), 32–45.